**International Conference on Estuaries and Coasts**
**November 9-11, 2003, Hangzhou, China**

# NUMERICAL STUDIES OF THE CIRCULATION IN THE YELLOW SEA AND EAST CHINA SEA

Kun LEI
Chinese Research Academy of Environmental Sciences, Beijing 100012, China,
E-mail: leikun@craes.org.cn

Wenxin SUN & Guimei LIU
Institute of Physical Oceanography, Ocean university of China, Qingdao 266003, China

**Abstract:** The Lagrangian circulation in the Yellow Sea and East China Sea is simulated numerically with a dynamic model based on the Lagrangian theory. Comparisons between the model results and the observations show reasonable agreements. The results indicate that the circulation in The Yellow Sea exhibits large variability in winter and summer, while the circulation in the East China Sea remains relatively stable. The difference originates from the variations of the driving mechanisms of the circulation. For the Yellow Sea, the circulation pattern is dominated by the wind force in winter, but by the coaction of baroclinic gradient force and tidal force in summer. For the East China Sea, however, the boundary force is the dominant factor in both winter and summer, and therefore has similar impact on the circulation pattern.

**Key words**: Lagrangian circulation, The Yellow Sea and East China Sea, Simulation

## 1. INTRODUCTION

The Yellow Sea and East China Sea (YSECS) is an open marginal sea in the west of the northern Pacific Ocean with complicated topographic variations (Fig.1). The circulation in the YSECS is the result of the low-frequency (or intertide) circulation, tidal current, wind, heat fluxes in the sea surface and the nonlinear interactions between the flow produced by these factors and the bottom topography. Located in the East Asian monsoon area, the wind and heat fluxes in the sea surface show dramatic seasonal variations. Consequently, the circulation in the YSECS varies both with the tide and the seasons.

Large quantities of studies (Hu D.X., 1994; Fang Y. et al, 1997; Tetsuo Y. et al, 1997), both observational and numerical, have been done on the circulation in the YSECS, and the general features of the circulation has been reviewed and sketched as a conceptual picture (Fig.2)(Guan, 1994), where the YSECS circulation consists of two current systems, the warm and saline current of oceanic origin (Kuroshio and its branches, Tsushima Warm Current, Taiwan Warm Current, Yellow Sea Warm Current) and the less saline littoral current system, although there still are some controversies.

The Lagrangian observations in the YSECS are scarce in quantity and limited in temporal-spatial scale (Tang Y.X. et al, 2000), and therefore is difficult to give a general Lagrangian circulation pattern yet. In comparison with observations, the numerical studies on the Lagrangian circulation are fruitful relatively. Feng and Wu (1995), Feng et al (1996) and Feng S. (1998) propose a model, which describe the circulation in the coastal sea system in a weakly nonlinear regime where both tidal currents and some quasi-steady flows, such as the Kuroshio in the East China are dominant and in the same order. The model has been used in the studies of many coastal areas and bays, and got satisfying results (Sun W.X., 1989; Dortch M.S. et al, 1992). A scale analysis of this model has been done to get the Lagrangian model

suitable to the Yellow Sea and the East China Sea (YSECS) (Sun W.X. et al, 2000). The objective of this work is to describe the Lagranian circulation in the YSECS and its driving mechanisms by numerical modeling base on the model (Sun W.X. et al, 2000). The results will be significant for determining the transport and exchange of water, materials and biota in the YSECS.

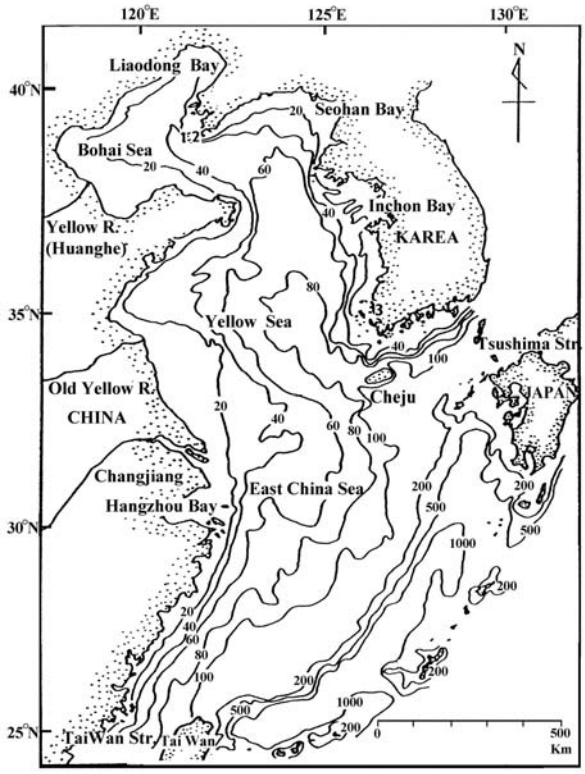


**Fig. 1** The map of the Bohai Sea, the Yellow Sea and the East China Sea (Numbers show the depth in meter)

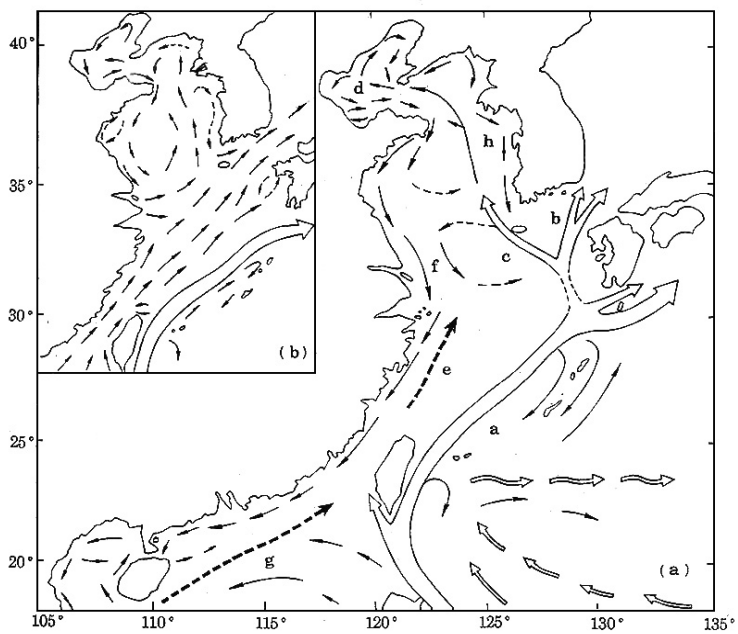


**Fig. 2** Schematic representations of the major current systems in the Bohai, Huanghai, East China seas and adjacent areas for winter (a) and for summer (b) (from Guan, B.X., 1994)
a: Kuroshio; b: Tsushima Warm Current; c: Yellow Sea Warm Current; d: Bohai Circulation; e: Taiwan Warm Current; f: China Coastal Current; h: West Korea Coastal Current

## 2. DESCRIPTION OF THE MODEL

The model (Sun W.X. et al, 2000) is simplified here to a diagnostic model under the condition of ignoring the nonlinear interaction between the current field and the thermohaline field and solves for the solid surface and three components of the current field A short description of the model is given as follow, but more details can be found in Sun W.X. et al (2000) .

Zero order model:

$$\nabla \cdot \vec{u}_0 = 0 \tag{1}$$

$$-fv_0 = -g\frac{\partial \zeta_0}{\partial x} - \frac{g}{\rho_0}\frac{\partial}{\partial x}\int_z^0 \rho' dz' + \frac{\partial}{\partial z}(\upsilon \frac{\partial u_0}{\partial z}) \tag{2}$$

$$fu_0 = -g\frac{\partial \zeta_0}{\partial y} - \frac{g}{\rho_0}\frac{\partial}{\partial y}\int_z^0 \rho' dz' + \frac{\partial}{\partial z}(\upsilon \frac{\partial v_0}{\partial z}) \tag{3}$$

$$\rho = \rho_0 + \rho'(T,S) \tag{4}$$

$z = 0$:

$$\upsilon \frac{\partial (u_0, v_0)}{\partial z} = 0 \tag{5}$$

$$w_0 = 0 \tag{6}$$

$z = -h$:

$$\upsilon \frac{\partial (u_0, v_0)}{\partial z} = k(u_0, v_0) \tag{7}$$

$$w_0 = -\vec{u}_0 \cdot \nabla h \tag{8}$$

Solid boundary:

$$\int_{-h}^0 \vec{u}_0 \cdot \vec{n} dz = 0 \tag{9}$$

Open boundary:

$$\int_{-h}^0 \vec{u}_0 \cdot \vec{n} dz = Q \tag{10}$$

One order model:

$$\nabla \cdot \vec{u}_1 = 0 \tag{11}$$

$$-fv_1 = -g\frac{\partial \zeta_1}{\partial x} - \frac{g}{\rho_0}\frac{\partial}{\partial x}\int_z^0 \rho' dz' + \frac{\partial}{\partial z}(\upsilon \frac{\partial u_1}{\partial z}) + \pi_1 - \vec{u}_0 \cdot \nabla u_0 \tag{12}$$

$$fu_1 = -g\frac{\partial \zeta_1}{\partial y} - \frac{g}{\rho_0}\frac{\partial}{\partial y}\int_z^0 \rho' dz' + \frac{\partial}{\partial z}(\upsilon \frac{\partial v_1}{\partial z}) + \pi_2 - \vec{u}_0 \cdot \nabla v_0 \tag{13}$$

$$\rho = \rho_0 + \rho'(T,S) \tag{14}$$

$z = 0$:

$$w_1 = 0 \tag{15}$$

$$\upsilon \frac{\partial (u_1, v_1)}{\partial z} = (\tau_x, \tau_y) \tag{16}$$

$z = -h$:

$$w_1 = -\vec{u}_1 \cdot \nabla h \tag{17}$$

$$\upsilon \frac{\partial (u_1, v_1)}{\partial z} = k(u_1, v_1) \tag{18}$$

Solid boundary:

$$\int_{-h}^0 \vec{u}_1 \cdot \vec{n} dz = 0 \tag{19}$$

Open boundary (inflows):

$$\int_{-h}^0 \vec{u}_1 \cdot \vec{n} dz = 0 \tag{20}$$

where $u,v$ is the velocity components of $x,y$ direction; $\zeta$ is water level; $h$ is the undisturbed water depth; $f$ is the coriolis force parameter; $g$ is the gravity acceleration; $\upsilon$ is the eddy viscosity; $k$ is the bottom friction coefficient; $\tau_a$ is the wind stress in the surface; $\pi_1, \pi_2$ is the

tidal force; $v_n$ is the normal velocity at the boundary; $Q$ is the unit discharge at the open boundary。All of the variables mentioned above are the long-term time averaged Lagrangian variables.

## 3. NUMETICAL METHODS

With the vertical σ coordinate transformation:

$$\sigma = \frac{h+z}{h} \qquad \sigma \in [0,1] \tag{21}$$

and the assumption:

$$\upsilon = \upsilon_0(x,y)\mu(\sigma) \tag{22}$$

($x, y, z$)coordinate system can be changed to the ($x, y, \sigma$)coordinate system. In the right-handed σ coordinate system:

$$\sigma = \begin{cases} 0 & z = -h \quad (Bottom) \\ 1 & z = 0 \quad (Surface) \end{cases} \tag{23}$$

After the coordinate change, the equations are reformulated in a new coordinate system. With $q_0 = u_0 + iv_0$ and $q_1 = u_1 + iv_1$, the equation can be expressed as complex:

Zero order model:

$$\frac{\partial}{\partial\sigma}(\mu\frac{\partial q_0}{\partial\sigma}) - i\frac{fh^2}{\upsilon_0}q_0 = \frac{gh^2}{\upsilon_0}\Gamma + \frac{gh^2}{\upsilon_0}G \tag{24}$$

$$\sigma = 1: \quad \mu\frac{\partial q_0}{\partial\sigma} = 0 \tag{25}$$

$$\sigma = 0: \quad \frac{\upsilon}{h}\frac{\partial q_0}{\partial\sigma} = kq_0 \tag{26}$$

Where:

$\Gamma = \frac{\partial\zeta_0}{\partial x} + i\frac{\partial\zeta_0}{\partial y}$; $G = (\frac{\partial b}{\partial x} + \frac{1-\sigma}{h}\frac{\partial h}{\partial x}\frac{\partial b}{\partial\sigma}) + i(\frac{\partial b}{\partial y} + \frac{1-\sigma}{h}\frac{\partial h}{\partial y}\frac{\partial b}{\partial\sigma})$; $b = h\int_\sigma^1 \rho' d\sigma$

One order model:

$$\frac{\partial}{\partial\sigma}\left(\mu\frac{\partial q_1}{\partial\sigma}\right) - i\frac{fh^2}{\upsilon_0}q_1 = \frac{gh^2}{\upsilon_0}\Gamma + \frac{h^2}{\upsilon_0}\pi + \frac{h^2}{\upsilon_0}F + \frac{gh^2}{\upsilon_0}G \tag{27}$$

$$\sigma = 1: \quad \mu\frac{\partial q_1}{\partial\sigma} = \frac{\tau_a h}{\rho_0\upsilon_0} \tag{28}$$

$$\sigma = 0: \quad \mu\frac{\partial q_1}{\partial\sigma} = \frac{kh}{\upsilon_0}q_1 \tag{29}$$

where: $\pi = \pi_1 + i\pi_2$, $F = (\vec{U}_0 \cdot \nabla U_0 + i\vec{U}_0 \cdot \nabla U_0)$

Based on the current splitting method (Sun W.X., 1992; Sun W.X. et al, 2000), the $q_0$ can be split into barotropic current induced by the boundary force, baroclinic gradient current, and $q_1$ can be split into components: barotropic current induced by the boundary force, baroclinic gradient current, wind-driven current, tide-induced current, coupling of zero-order current.

$$q_0 = \frac{gh^2}{\upsilon_0}\Gamma P_1^0(\sigma) + \frac{gh^2}{\upsilon_0}P_2^0(\sigma) \tag{30}$$

$$q_1 = \frac{gh^2}{\upsilon_0}[\Gamma P_1(\sigma) + P_2(\sigma) + P_3(\sigma) + P_4(\sigma)] + \frac{\tau_a h}{\rho_0\upsilon_0}P_5(\sigma) \tag{31}$$

Calling (30, 31) into (24-29), the profile functions of velocity components can be obtained:

$$\frac{\partial}{\partial\sigma}(\mu\frac{\partial p_j}{\partial\sigma}) + ik^2 p_j = \varphi_j \tag{32}$$

$$\sigma = 1: \quad \mu\frac{\partial p_j}{\partial\sigma} = \psi_j \tag{33}$$

$$\sigma = 0: \quad \mu \frac{\partial p_j}{\partial \sigma} = \frac{kh}{\upsilon_0 \rho_0} p_j \tag{34}$$

in which $k^2 = -\frac{fh^2}{\upsilon_0}$, $\varphi_j = \begin{cases} 1 \\ G \\ \pi / g \\ F / g \\ 0 \end{cases}$, $\psi_j = \begin{cases} 0 \\ 0 \\ 0 \\ 0 \\ 1 \end{cases}$, $j = \begin{cases} 1 \\ 2 \\ 3 \\ 4 \\ 5 \end{cases}$.

These profile functions are related to the known parameters $(\mu, \upsilon_0, f, h)$ and the forces $(\pi, F, G)$ only, and can be solved respectively.

The model's domain covers the Bohai Sea, Yellow Sea and the East China Sea with a horizontal resolution of 5′×5′ and the non-uniformly spaced vertical grid. The model is initialized with temperature and salinity field and is forced by the seasonally mean wind and the inflow. To take into account for the river discharge, we introduce the fresh water from the Changjiang River. The fluxes at the open boundary are list in Table 1.

**Table 1** The flow distribution at the open boundaries

| Open Boundary | Flux in winter (sv) | Flux in summer(sv) |
|---|---|---|
| Taiwan Strait | +1.0 | +2.0 |
| The Kuroshio area to the east of the Taiwan | +22.5 | +25.7 |
| Tokara Strait | -21.0 | -24.2 |
| Tsushima strait | -2.5 | -3.5 |
| Changjiang esauaty | +0.01 | +0.09 |

Note: "+" means inflow; "-" means outflow

## 4. CIRCULATION PATTERN OF THE EAST CHINA SEA AND YELLOW SEA

With the model mentioned above, a diagnostic numerical calculation of the Lagrangian circulation in the YSECS was made. The general features of the simulated circulation and the water mass transport were introduced herein.

### 4.1 THE CIRCULATION IN WINTER

The sea surface circulation and the depth-averaged circulation are illustrated in Fig3, 4. The oceanic origin subsystem of the circulation, or Kuroshio and its branches and extensions, flow northward or northeastward, while the coastal subsystem flow southward along the coastal line. In the Yellow Sea, the Yellow coastal current originate from the water flowing out of the Bohai Sea along the coastal line through the western part of the Bohai strait. The Yellow sea warm current intrudes northwards to the Yellow Sea from the southwest of the Cheju Island. Few of the Yellow warm current flows into the Bohai sea, but most of them turn to the east and flow southward along the West Korea coast, forming the west Korea coastal current. The Yellow Sea coastal current flows southwards along the East China Sea coast and connects with the Minzhe coastal current. The results agree well with the field observation (Tang Y.X., 2000). In the East China Sea, the Taiwan Warm current, Kuroshio current, the Tsushima current flows northward in the shelf area, and constitute the East China Sea circulation.

### 4.2 THE CIRCULATION IN SUMMER

ComparingFig.5,6 with Fig.3,4, it can be found that the summer circulation regime in the East China sea is quite similar to that in winter, only the Minzhe coastal current reverse and flows southward along the coastal line. With the larger fluxes of inflow in the open boundary in summer, the Taiwan Warm current, Kuroshio current, and the Tsushima current are stronger in summer, but the flow regime still remain the same as that in winter. The summer

circulation pattern in the Yellow Sea is markedly different with that in winter. A pronounced anticyclonic eddy is formed in the Yellow Sea and almost no Yellow Sea Warm current can be found in summer and the intrusion to the Yellow sea. Therefore it is believed that Yellow Sea Warm current is very week in summer.

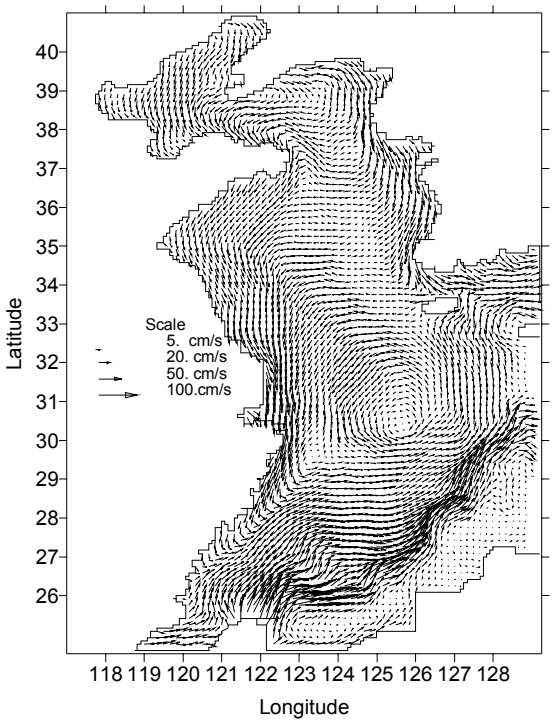


**Fig. 3** The surface circulation in the Yellow Sea and the East China Sea in winter

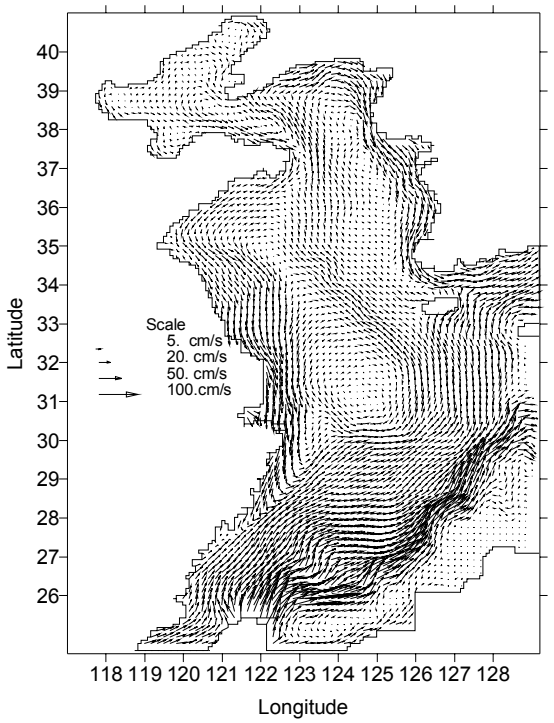


**Fig. 4** The depth-averaged circulation in the Yellow Sea and the East China Sea in winter

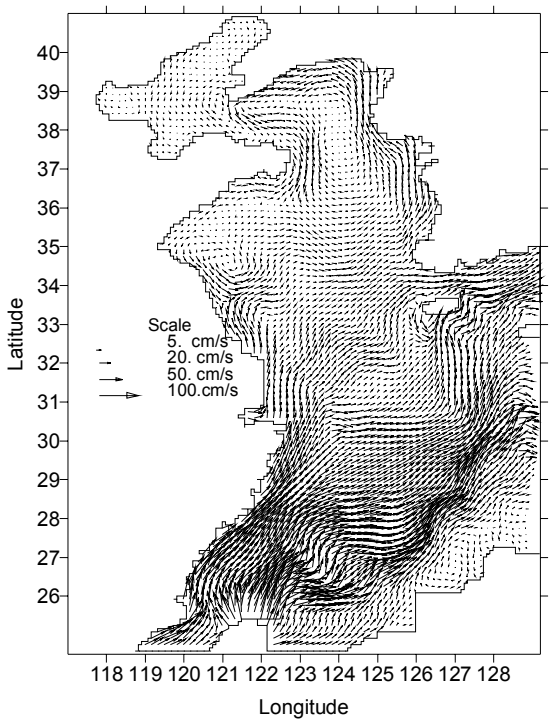


**Fig. 5** The surface circulation in the Yellow Sea and the East China Sea in summer

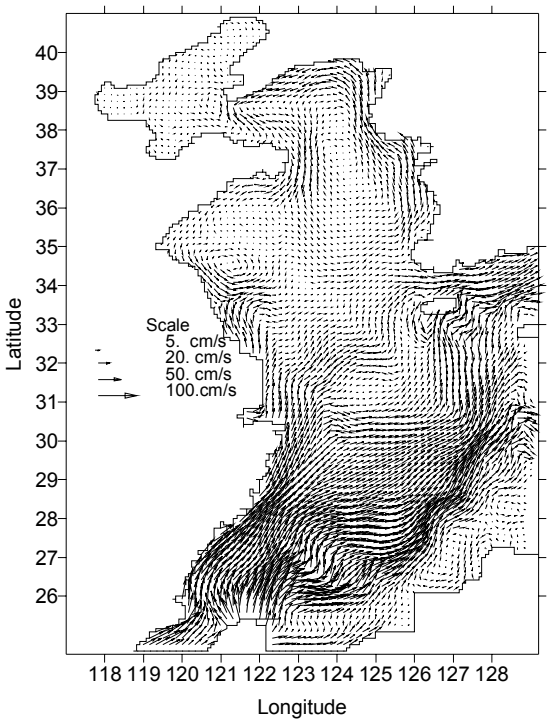


**Fig. 6** The depth-averaged circulation in the Yellow Sea and the East China Sea in summer

## 4.3 CURRENT COMPONENTS

Considering single driving forces, current induced by the wind, tidal force, baroclinic gradient force, inflow at the open boundary can be obtained respectively.

### 4.3.1 Wind-driven current

The wind stress mainly affects water movement in surface and the coastal areas. In the surface layer and the coastal areas, the simulated current (Fig.7) mainly follows the wind, forming strong northward coastal current in winter and southward coastal current in summer. In the greater depth of the outer area, however, the influence of wind stress decreases and the return (or compensatory) current can be found, with directions opposite to the wind.

### 4.3.2 Tide-induced current

The tide-induced current (Fig.8): Tide induced current is pronounced in coastal area, with a velocity of 10-15cm/s, while very weak in the shelf area with larger water depth. A distinct feature of the this component is the formation of a closed anticyclonic eddy in the Yellow Sea, implying that tidal residual is an important components of the Yellow Sea circulation in summer, supporting the conclusion that not only the "thermal" component, but also the "tidal" components contribute to the formation of the Yellow sea circulation in summer (Tang Y.X., 2000). Therefore, the model reveals that the high-frequency tidal forcing also generate important current through non-linear mechanisms. And the nonlinearity increases with tidal current amplitude, therefore are greatest in coastal areas.

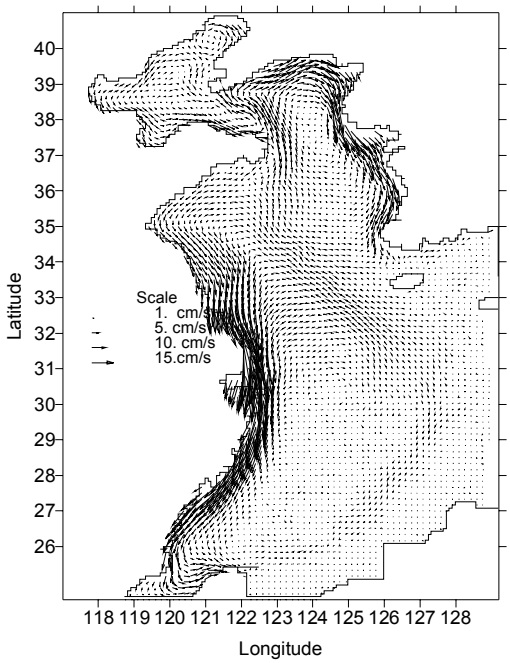


**Fig. 7** The depth-averaged wind-driven current in the Yellow Sea and the East China Sea in winter

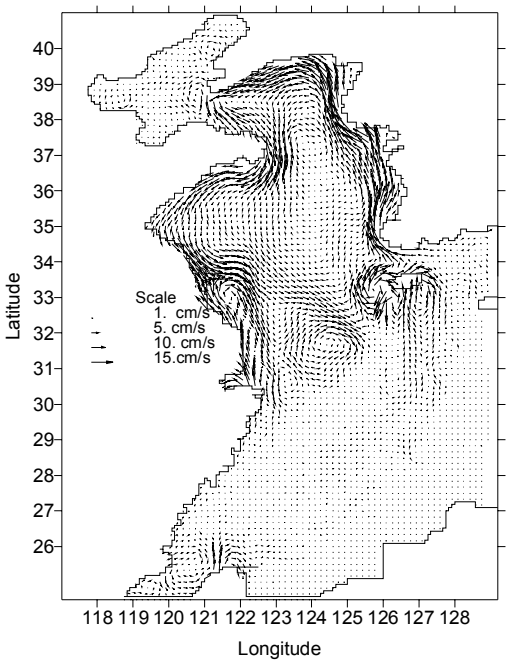


**Fig. 8** The depth-averaged tide-induced current in the Yellow Sea and the East China Sea in winter

### 4.3.3 Baroclinic gradient current

The baroclinic contribution to the circulation can be found in Fig.9, 10. With a velocity of 10-15cm/s and the same flowing direction of Taiwan Warm Current and the Kuroshio Current, the baroclinic gradient current contribute significantly and is an important component of the East China Sea circulation. In the Yellow Sea, however, the gradient current is very weak in winter, while pronounced in summer, forming a closed eddy in the Yellow Sea, and is an essential component for the formation of the Yellow Sea circulation in summer.

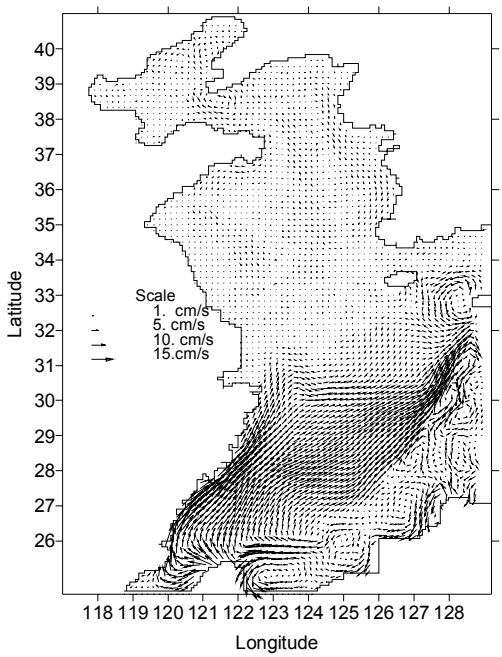


**Fig. 9** The depth-averaged thermohaline current in the Yellow Sea and the East China Sea in winter

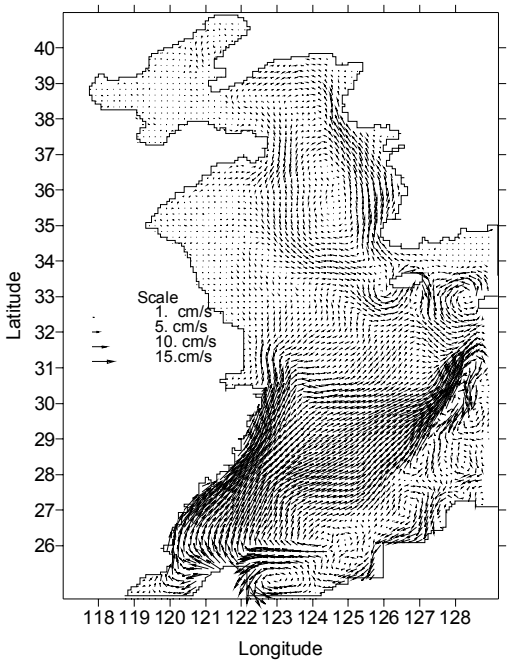


**Fig. 10** The depth-averaged thermohaline current in the Yellow Sea and the East China Sea in summer

### 4.3.4 Inflow at the open boundary

The circulation driven by the inflow at the open boundary namely is the zero-order barotropic circulation (Fig.11, 12). It can be found that the current induced by the inflow from the Taiwan Strait and the area east of the Taiwan Island mainly affects the circulation pattern of the East China Sea, has little influence on the circulation in the Yellow Sea. With the inflow, the northward-flowing Taiwan Warm Current, the northeastward-flowing Kuroshio Current along the shelf edge, and the Tsushima Warm Current constitute the general pattern of the circulation in the East China Sea.

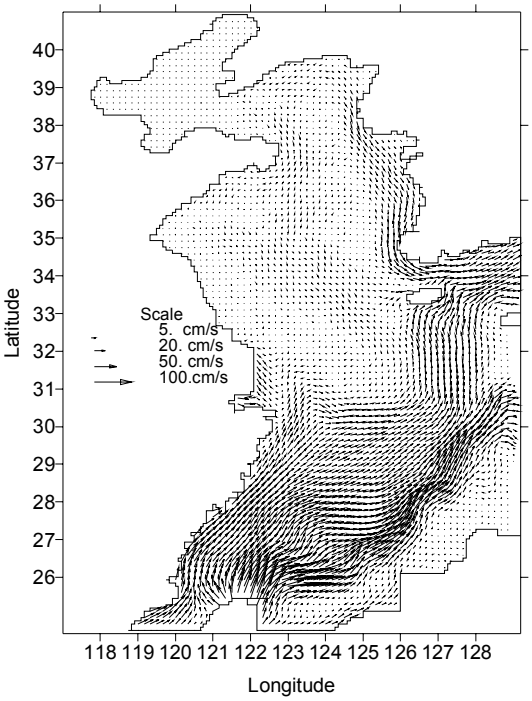


**Fig. 11** The depth-averaged barotropic current in the Yellow Sea and East China Sea in winter

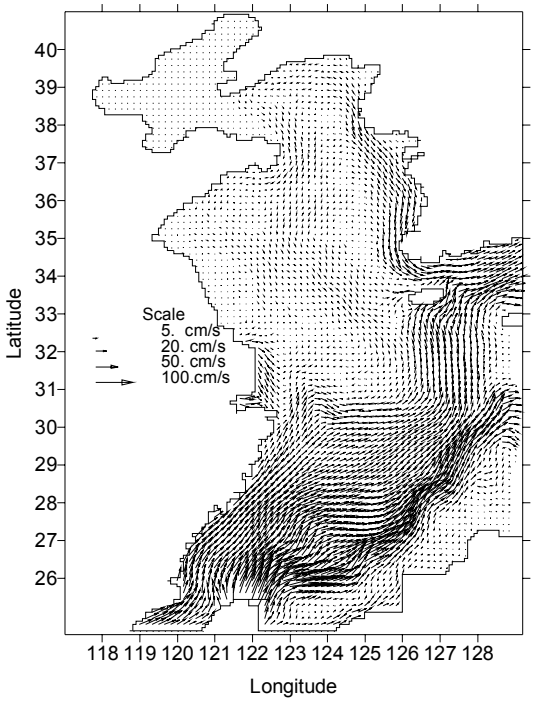


**Fig. 12** The depth-averaged barotropic current in the Yellow Sea and East China Sea in summer

## 4.4 THE DRIVING MECHANISMS OF THE CIRCULATION IN THE YELLOW SEA AND EAST CHINA SEA

If comparing the overall circulation (Fig.3-6) with the currents components (Fig.7-12), the relative significance of currents components mentioned above can be analyzed respectively. It can be found that the circulation in the East China Sea is dominated by the boundary force induced by the inflow at the boundary, and the baroclinc gradient and wind force also contribute to the circulation of the circulation pattern to certain extent. The dramatic changes of the circulation in the Yellow Sea are the result of the turn of different driving forces. The circulation in summer is the results of the cooperation of the tidal force and the baroclinic gradient force. The circulation in winter, however, is dominated by the wind force. The seasonal variability of wind has substantial residual effect in the circulation pattern.

## 5. CONCLUSIONS

The circulation in the Yellow Sea changes exhibits large variability in winter and summer. The circulation in winter is featured by the southward coastal current and the northward Yellow Sea warm current, but is characterized in summer by the closed anticyclonic meander. The circulation in the East China Sea remains relatively stable through the year except the Minzhe coastal current, which reverses in winter and summer. In the Yellow Sea, wind is the dominant driving force in winter; the tidal force and the baroclinic gradient force are the prevailing factor in summer. In the East China Sea, however, boundary force is the significant mechanisms both in the winter and summer season.

## REFERENCES


Dortch, M.S., Chapman R.S. and Steven R.A., Members, ASEC., 1992. Application of three-cimensional Lagrangian residual transport, *J. Hydraulic Engineering*, Vol.118, No.6. pp.831-848.

Fang, Y., Zhang, Q.H., and Fang, G.H., 1997. A numerical study on the path and origin of the Yellow Sea Warn Current, *The Yellow Sea*, Vol.3, pp. 18-26.

Feng S, 1998. On circulation in Bohai sea, Yellow Sea and East China Sea. Health of the Yellow Sea. Hong G.H., Zhang J. and Park B.K. (Editors), Soul, The Earth Love Publication Association. PP.41-77.

Feng S. and Wu D., 1995. An inter-tidal transport equation coupled with turbulent $k-\omega$ model in a tidal and quasi-steady current system. *Chinese Science Bulletin*, Vol.39, No.6, pp. 136-139.

Feng S., Wu D., Wang H. et al., 1996. A generalized set of equations for coastal ocean circulation. *8th Intern. Biennial Conf. on physical of estuaries and coastal seas*, the Hague, the Netherlands.

Guan, B.X., 1994. Patterns and structures of the currents in Bohai, Huanghai and East China Seas. Oceanology of China Seas, Vol.1, Zhou Di, Liang YuanBo and Zeng ChengKui (Editors), Kluwer Academic Publishers, pp.17-26.

Hu D.X., 1994. Some striking features of circulation in Huanghai Sea and East China Sea. Oceanology of China Seas. Vol.1, Zhou Di, et al (Editors), Kluwer Academic Publisher, pp. 27-38.

Sun W.X., 1992. Current splitting method- a numerical method of the 3-D hydrodynamics in shallow seas. The Numerical Calculations in Physical Oceanographies. Feng S.Z. and Sun W.X. (Editors), Henan Technology Press, pp. 100-195.

Sun W.X., Liu G.M. and Jiang W.S et al., 2000. The numerical studies of circulation in the Yellow sea and East China Sea I. The numerical circulation model in the Yellow Sea and East China Sea. *Journal of ocean university of Qingdao*, Vol. 30, No. 3, pp. 369-375.

Sun, W.X., Xi, P .G. and Song, L.N., 1989. Three-dimension tide-induced Lagrange esidual circulation in the Bohai Sea, *Journal of ocean university of Qingdao*, Vol. 19, No.2, pp.27-35.

Tang Y. X. Zou E.M., Li H.J. et al., 2000. Some features of circulation in the southern Huanghai Sea. *ACTA Oceanologica Sinaca*, Vol.22, No.1, pp. 1-16.

Tetsuo Y., Akihiko M. and Kaour I., 1997. Seasonal variation in surface circulation of the East China Sea and the Yellow Sea from the satellite altimetric data. *Continental Shelf Research*, Vol.17, No.6, pp.655-664.